

ROLE OF MODERATE SINTERING TEMPERATURE ON REDUCING TIN DIFFUSION AT TiO₂/TCO INTERFACE

M. RAICOPOL^a, E. VASILE^b, C. DASCALU^{c*}, R. ATASIEI^c

^a*Department of Organic Chemistry, University Politehnica of Bucharest, Bucharest, Romania.*

^b*Faculty of Medical Engineering, University Politehnica of Bucharest, Bucharest, Romania.*

^c*Department of Physics, University Politehnica of Bucharest, Bucharest, Romania.*

Evaporation induced self-assembly (EISA) technique was used to fabricate nanostructured titanium dioxide (TiO₂) films. Using lyotropic liquid crystals as templates for growing mesoporous thin films on conducting transparent electrodes (TCO) only moderate temperatures are necessary for template removal. Nanoscale analysis of the cross-sectional structure and composition of TiO₂ deposited on fluorine doped tin oxide coated glass (FTO) has shown that no tin diffusion is present in the titania film, contrary to what happens when higher temperatures are used with other techniques for growing TiO₂ films. The lack of tin contamination within EISA technique prevents an irreversible transition from metastable anatase – generally considered to exhibit superior electrode performance – to the equilibrium rutile phase.

(Received September 25, 2013; Accepted November 21, 2013)

Keywords: EISA, thin film, TiO₂, TCO, EDAX

1. Introduction

During the last two decades, substantial efforts have been paid to obtain high quality nanostructured titanium dioxide thin films, due to their numerous applications in photocatalysis [1], gas sensing [2], self cleaning coatings [3], self sterilizing coatings [4] and, very promising, in the field of renewable energy [5]. Dye-sensitized solar cells (DSSCs) appear to be an attractive alternative to conventional solid-state photovoltaic devices because they offer the possibility of inexpensive and efficient solar energy conversion [5-8]. Highly efficient DSSCs with photoanodes prepared from organized mesoporous TiO₂ were reported by Grätzel et al. as an alternative to nanoparticle photoanodes with similar efficiencies but with more elaborate manufacturing procedures [9]. Titanium dioxide (known also as titania) occurs in two main phases: the thermodynamically stable rutile and the metastable anatase. Owing to its higher photoactivity [10], anatase, rather than rutile, is generally the preferred structure in building photoanodes for DSSCs, for instance. It also exhibits a higher conduction band edge than rutile. In a comparative study of rutile and anatase a key factor for the better photocatalytic performances of the later is given by its larger surface area leading to a higher density of surface-adsorbed species [11]. One of the best methods employed for the synthesis of inorganic coatings with controlled porosity is the evaporation-induced self-assembly (EISA). The first step of the synthetic protocol for EISA consists in applying on a substrate a homogenous solution of inorganic precursor containing surfactants, water, an acid catalyst and an organic solvent (usually an alcohol). The initial

*Corresponding author: dascaluc@yahoo.com

concentration of the surfactant is chosen below the critical micelle concentration (CMC). Upon evaporation of the organic solvent, the CMC is exceeded and the surfactant micelles self-assemble forming lyotropic mesophases. In the following step, the substrate is kept under controlled temperature and humidity conditions and due to hydrolysis and polycondensation reactions of the inorganic precursor an inorganic network grows around the liquid crystalline phase. During the final thermal treatment step the surfactant template is removed leading to well-defined mesostructured materials [12].

Owing to their good electrical and optical properties, tin-doped indium oxide films (ITO) on glass substrates have been used in many optoelectronic applications as transparent electrodes [13]. It has been shown that exposure of ITO to high temperatures during the thermal treatment step necessary for the synthesis of photoanodes leads to indium diffusion into the TiO₂ layer, thus reducing the conductivity of the former [14]. Therefore, the material most commonly used as substrate for the fabrication of photoanodes is fluorine-doped tin oxide coated glass (FTO).

However a recent study [15] has shown that at the temperatures required for the sintering step necessary in the manufacturing of conventional anatase nanoparticle photoanodes (i.e. 450°C - 600°C), tin from the TCO migrates into the TiO₂ layer leading to an alteration of the electrode composition, which can have a detrimental effect on devices functioning. When using titania as photoanodes for solar cells, anatase is generally considered to exhibit superior performance than rutile [16,17]. However, an irreversible transition from metastable anatase to the equilibrium rutile phase is reported to start at temperatures from 600-700°C and is accelerated beyond this temperatures [18]. The presence of certain unintentional impurities in TiO₂ can also induce the phase transformation of anatase to rutile allowing this process to occur at lower temperatures [11,18].

Because mesoporous films grown using lyotropic liquid crystals as templates require only moderate temperatures for template removal, a study dealing with the diffusion of impurities from the TCO layer into mesoporous anatase photoanodes could bring further insight into the feasibility of employing EISA for the manufacturing of titania films.

In this paper we report our results concerning the characterization of mesoporous anatase films grown onto FTO transparent conducting oxide electrodes following the EISA synthetic approach and a subsequent calcination step at 360°C. Using EISA technique for preparing the nanoporous structured thin films of TiO₂ we show that no diffusion of tin into the active photoanode layer exists, contrary to what has been observed when higher temperature were used for manufacturing the electrodes [11]. In Section 2 the experimental method for preparing the TiO₂ layer is described. In Section 3 the experimental results concerning the structural characterization of the thin titania films are reported. The last section is devoted to the conclusions.

2. Experimental

Pluronic 123, titanium (IV) ethoxide, hydrochloric acid 37% and 1-butanol were purchased from Aldrich. Commercially available FTO/glass substrates with a sheet resistance of 7 Ω per square (Solaronix) were thoroughly cleaned in an ultrasonic bath successively with detergent solution, deionized water and 2-propanol and rinsed with deionized water.

For the synthesis of meso-TiO₂ layers, a titania precursor solution was obtained by slowly adding under stirring concentrated hydrochloric acid (1.4 mL) over titanium (IV) ethoxide (2.1 g); separately, a surfactant solution was prepared by dissolving Pluronic 123 (0.65 g) in 1-butanol (7.4 mL) and then mixed with the HCl/Ti(EtO)₄ solution. The resulting mixture was stirred at room temperature for 3 hours and spin-coated onto FTO/glass substrates (2400 rpm, 20 s). The coated substrates were aged for 2 days at 20°C and 80 % relative humidity and finally calcined in a muffle furnace at 360°C for 4 hours (heating rate of 1°C/min). Structural characterization of the synthesized films was carried out using grazing-incidence X-ray diffraction on a PanAlytical diffractometer with Cu-K_α radiation ($\lambda=1.54065$ Å). The morphology of the films was obtained

using a FEI high resolution transmission electron microscope (HRTEM) with an accelerating voltage of 300 kV and a FEI scanning electron microscope.

3. Results and discussions

For the synthesis of meso-TiO₂ thin films on FTO glass we have adopted the method developed by Ozin et al. [19]. Their procedure involves the use of a non-ionic amphiphilic triblock-copolymer (Pluronic 123) as template agent, titanium (IV) ethoxide as inorganic precursor and 1-butanol as organic solvent. In order to remove the template and achieve the crystallization of the anatase phase, the films were calcined at 360°C for 4 hours. The crystalline structure of the deposited films was confirmed by grazing-incidence X-ray diffraction, which is superior to conventional XRD techniques in the study of thin films. The corresponding wide angle diffraction pattern (Fig.1) for calcined titania films on FTO substrates clearly shows peaks in agreement with the anatase crystalline phase and tin oxide from the underlying transparent conducting layer.

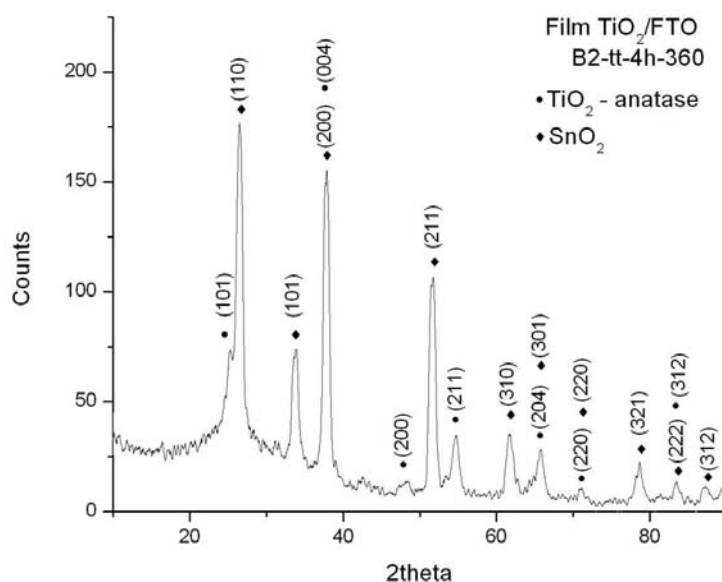


Fig.1 Grazing-incidence wide-angle diffraction pattern obtained from meso-TiO₂ film on FTO glass after calcination at 360 °C.

The scanning electron microscopy (SEM) has allowed to investigate the structural aspect of the surface TiO₂ thin film obtained by the sol-gel method. The SEM image for the surface of the synthesized films (Fig.2) reveals a uniform morphology with nanometer pores having diameters between 6 and 10 nm and round shaped TiO₂ nanocrystallites (diameter < 5 nm).

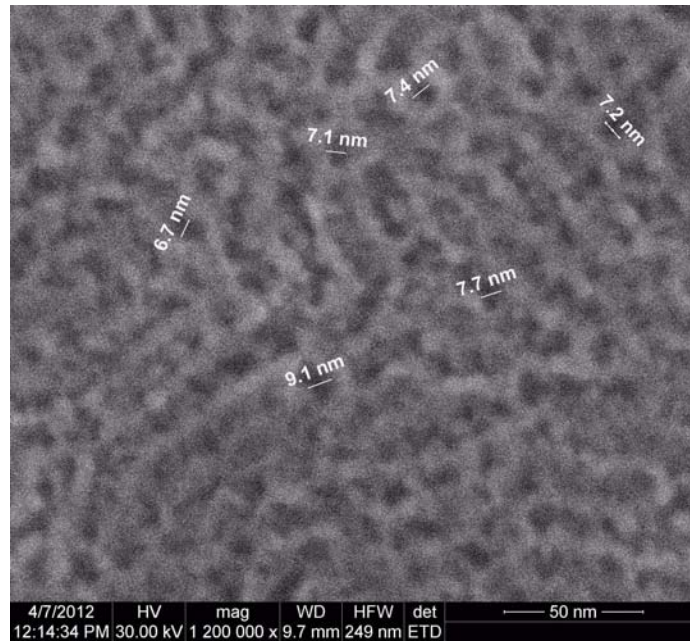


Fig.2. SEM secondary electron image of the surface of meso-TiO₂ film, magnification 1200000.

Structural investigations have been made in a transversal section of the multilayer thin film using electronic transmission microscopy (TEM). Elemental qualitative composition leading to the identification of the multilayer film regions has been carried by energy dispersive X-ray microanalysis (EDAX). The TEM image presented in Fig.3 shows the cross-section through the glass/FTO/TiO₂ structure. For the identification of different layers, EDAX spectra were collected in several points denoted 1-7. The top layer (1-3) is the active layer consisting of TiO₂ (anatase), followed by the TCO (SnO₂) layer (4). Underneath the TCO layer, a light contrast layer (5) containing mainly Si and O and a dark contrast layer (6) containing Sn and O were found, and finally the glass substrate (7).

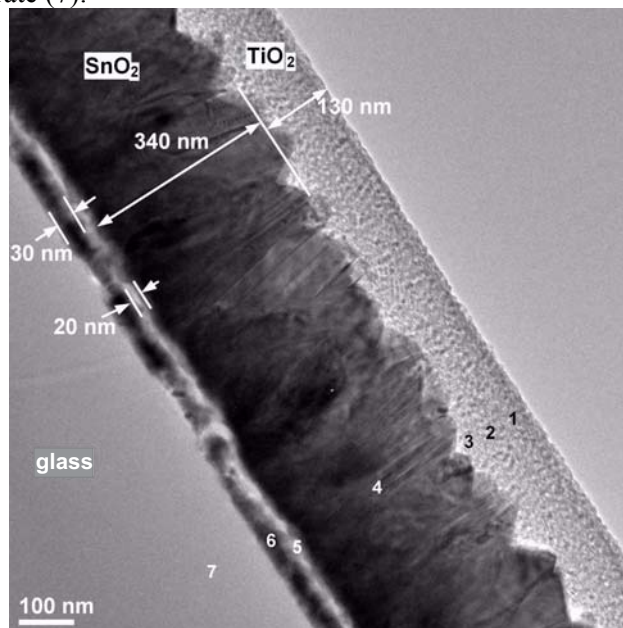


Fig.3. Bright field TEM image of the cross-section through the glass/FTO/TiO₂ multilayers.

In order to study the diffusion of tin from the FTO layer into the TiO_2 thin film, scanning transmission electron microscopy (STEM) and energy-dispersive X-ray microanalysis (EDAX) mapping were employed. The STEM image presented in Fig.4, where the contrast is related to the atomic number ("Z-contrast"), shows the layer structure of the interface. The brighter area contains the element Sn and the darker region at the top contains mainly Ti. These assumptions are confirmed by the EDAX elemental maps for Ti, Sn, Si and O also shown in Fig.4. Because the distribution of Ti and Sn reveal clearly a sharp interface between meso- TiO_2 and TCO layers, we can conclude that tin is not diffusing from the SnO_2 :F layer during the sintering process necessary for the synthesis of mesoporous titania film. This is in contrast with the results presented by Zerulla et al [15], which observed the diffusion of tin into nanocrystalline TiO_2 layer after a sintering process at higher temperature.

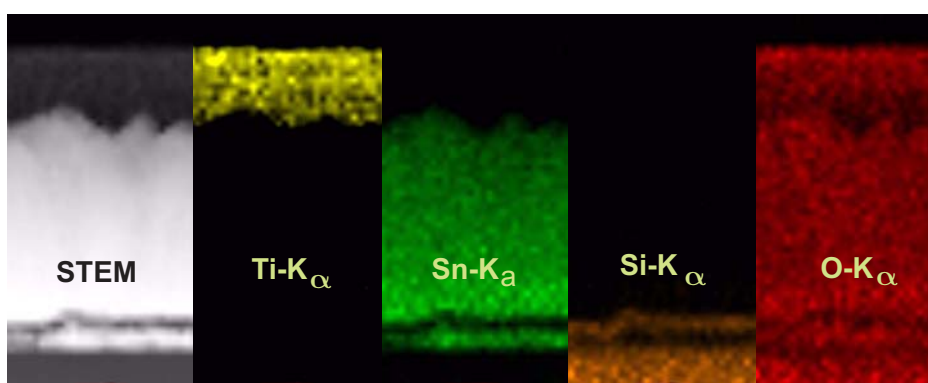


Fig.4. Scanning transmission electron microscopy image of the cross-section through the FTO/ TiO_2 thin films and corresponding elemental distribution maps for Ti, Sn, Si and O.

From the spatial distribution of the elements Ti, Sn and Si across the electrode, which is depicted in Fig.4 it is also evident that a sharp separation between Ti and Sn exists in the meso- TiO_2 /TCO interface; thus we can conclude that tin is not diffusing from the TCO layer during the sintering process performed at lower temperature.

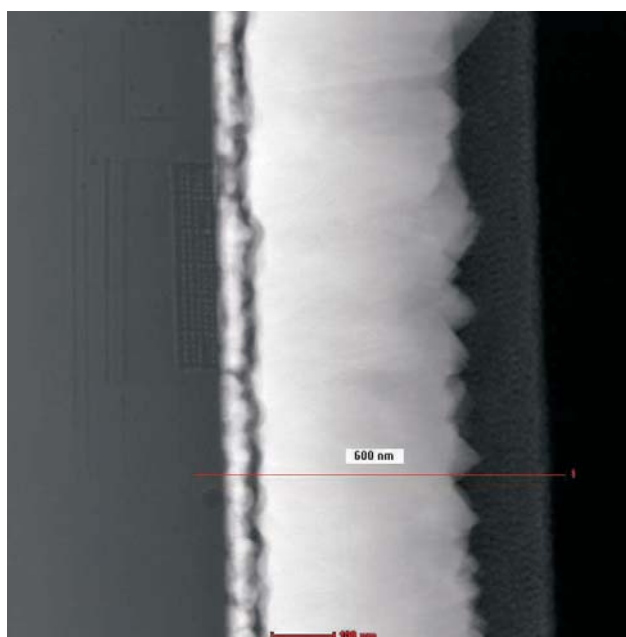


Fig.5. TiO_2 / SnO_2 /glass cross section and the line along which the elements were recorded.

The elemental line distribution recorded in the STEM-EDAX mode, along the cross sectional $\text{TiO}_2/\text{SnO}_2/\text{glass}$ ensemble, is presented in Figs.5 and 6. STEM image from Fig.5 highlights the $\text{TiO}_2/\text{SnO}_2/\text{glass}$ cross section and the line along which the elements were recorded, the distribution of which are shown in Fig.6. The distribution of the characteristic X-ray intensities Si-K_α , Ti-K_α and Sn-K_α are roughly proportional to the elements concentration along the line. It is observed that the Sn concentration presents a maximum at the interface with glass, followed by a minimum, then increase, and is rather constant in the region of the SnO_2 film (white contrast in Fig.5). In the TiO_2 zone (grey contrast in Fig.5) Sn concentration is minimum, as like as in the glass zone, therefore in the glass and in TiO_2 zones the element Sn is missing.

The Ti-K_α characteristic X-ray intensities present a maximum in the grey region (TiO_2 film) and a minimum in other zones. The Si-K_α characteristic X-ray intensities present a maximum in the left side of Fig.6 (glass zone) and a maximum inside the white region (white zone of Fig.5) at the glass/ SnO_2 interface. Also, in the rest of SnO_2 and TiO_2 regions the intensity of Si-K_α characteristic X-ray is minimum.

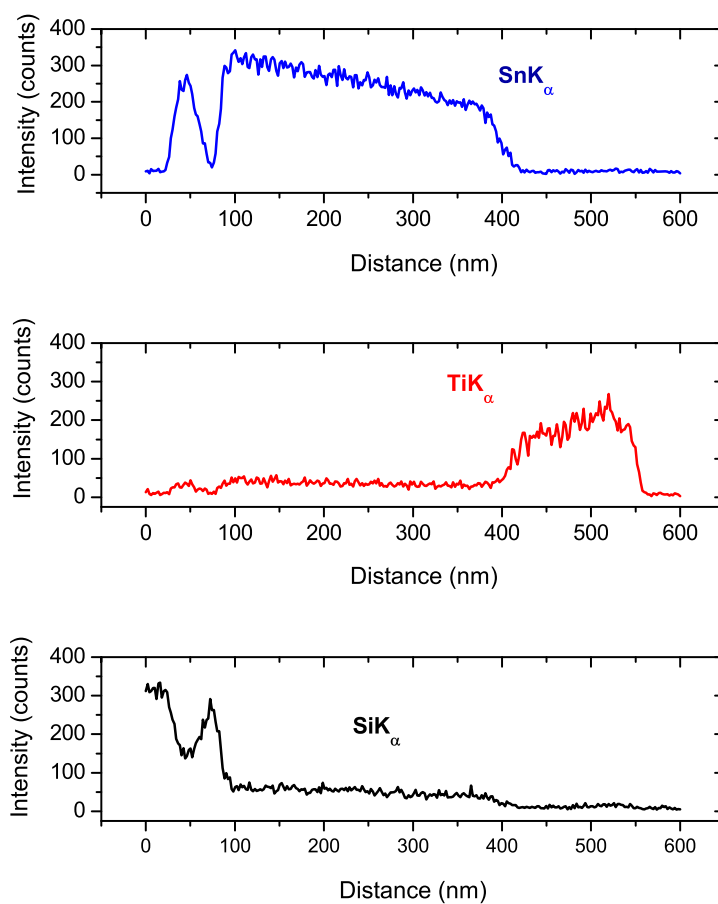


Fig.6. Elemental distribution profiles for Ti, Sn and Si across the TCO/ TiO_2 multilayers.

It can be seen that the Ti-K_α and Sn-K_α intensities drop rapidly at the interface $\text{SnO}_2/\text{TiO}_2$ film, which revealed that Sn is not diffusing in the TiO_2 area and Ti is not diffusing in the SnO_2 area.

4. Conclusions

High resolution electron microscopy techniques, as SEM, TEM, STEM and energy dispersive X ray microanalysis (EDAX) were employed to investigate the microstructure and the properties of anatase titania films prepared on FTO glass by the EISA technique. In very good agreement, both STEM and EDAX results reveal a sharp separation between the meso-TiO₂ and the FTO layers. Thus, it was shown that no diffusion of tin into the active TiO₂ layer occurs if the sintering process during the manufacturing of the electrodes is performed at lower temperatures (i.e. 360 °C). This temperature is sufficient for removing the template used for the synthesis of mesoporous TiO₂ following the evaporation-induced self-assembly (EISA) approach. Therefore, besides their enhanced performances, titania films seem to offer another advantage: their manufacturing process requires lower sintering temperatures and as such diffusion of impurities from the underlying TCO layer is avoided. This observation is of peculiar interest since anatase is generally considered to exhibit superior photovoltaic performance than rutile and tin doping has experimentally been proven to promote the anatase to rutile transformation at lower temperatures [11].

Acknowledgments

This work has been supported by a grant of Romanian National Authority for Scientific Research, CNCSUEFISCDI, project number PN-II-ID-PCE-2011-3-0535.

References

- [1] A. Fujishima, T.N. Rao, D.A. Tryk, *Journal of Photochemistry & Photobiology, C: Photochemistry Reviews*, **1**,1 (2000).
- [2] C. Carotta, M. Ferroni, V. Guidi, G. Martinelli, *Adv. Mater.*, **11**, 943 (1999).
- [3] A. Mills, S. Hodgen, S.K. Lee, *Res Chem Intermed.*, **31**, 295 (2004).
- [4] P. Hajkova, P. Spatenka, J. Horsky, I. Horska, A. Kolouch, *Plasma Processes and Polymers*, **4**, S397 (2007).
- [5] M. Grätzel, *Nature*, **414**, 338 (2001).
- [6] B. O. O'Regan, M. Grätzel, *Nature*, **353**, 737 (1991).
- [7] M. Sima, E. Vasile, A. Sima, *Digest Journal of Nanomaterials and Biostructures*, **8**(2), 757 (2013)
- [8] A. Hagfeldt, G. Boschloo, L. Sun, L. Kloo, H. Pettersson, *Chem. Rev.*, **110**, 6595 (2010).
- [9] M. Zukalová, A. Zukal, L. Kavan, M. Nazeeruddin, P. Liska, M. Grätzel, *Nano Lett.* **5**, 1789 (2005).
- [10] A. Scialfani, J.M. Herrmann, *J Phys. Chem.*, **100**, 13655 (1996).
- [11] D.A.H. Hanaor, C.C. Sorrell, *J Mater Sci.* **46**, 855 (2011).
- [12] C. Wang, D. Chen, X. Jiao, *Sci. Technol. Adv. Mater.*, **10**, 023001 (2009).
- [13] R.G. Gordon, *MRS Bull.*, **25**, 52 (2000).
- [14] S. Lee, J.H. Noh, S.T. Bae, I.S. Cho, J.Y. Kim, H. Shin, J.K. Lee, H.S. Jung, K.S. Hong, *J. Phys. Chem. C*, **113**, 7443(2009).
- [15] C. Andrei, T. O'Reilly, D. Zerulla, *Phys. Chem. Chem. Phys.*, **12**, 7241 (2010).
- [16] F.M. Rajab, D. Loaring, K.J. Ziegler, *Thin Solid Films*, **519**, 6598 (2011).
- [17] C.S. Karthikeyan, M. Thelakkat, M. Willert-Porada, *Thin Solid Films*, **511-512**, 187 (2006).
- [18] D.A.H. Hanaor, M.H.N. Assadi, S. Li, A. Yu, C.C. Sorrell, *Computational Mechanics*, **50**, 185 (2012).
- [19] S.Y. Choi, M. Mamak, N. Coombs, N. Chopra, G.A. Ozin, *Adv. Funct. Mater.*, **14**, 335 (2004).